Journal of Catalysis **202,** 89–99 (2001)
doi:10.1006/jcat.2001.3273, available online at http://www.idealibrary.com on IDEAL®

(Co)MoS_2/Alumina Hydrotreating Catalysts: An EXAFS Study of the Chemisorption and Partial Oxidation with O_2

J. T. Miller,*,[1] Christopher L. Marshall,† and A. J. Kropf†

*BP Research Center, E-1F, 150 Warrenville Road, Naperville, Illinois 60563; and †Chemical Technology Division, Argonne National Laboratory, Argonne, Illinois 60439

Received January 15, 2001; revised May 5, 2001; accepted May 5, 2001

The adsorption of O_2 on alumina-supported (Co)MoS_2 catalysts and the subsequent mild oxidation of the (Co)MoS_2 by O_2 have been studied by extended X-ray absorption fine-structure (EXAFS) spectroscopy. By analyzing the difference between spectra before and after O_2 exposure, small changes in the structure could be determined, which were not resolved using standard methods. At 20°C on MoS_2/alumina and (Co)MoS_2/alumina, O_2 is chemisorbed at the edge of the MoS_2 particles at a Mo–O distance of 1.73(2) Å. The O_2 chemisorption results at the Mo edge indicate that, despite the large fraction of Co at the surface of the MoS_2 crystallite in (Co)MoS_2/alumina, some of the Mo atoms are exposed to the reacting gases. At 100°C, there is partial substitution of S by O atoms in the Mo coordination sphere. The resulting decrease in both the Mo–S and Mo–Mo coordination numbers indicates partial disruption of the MoS_2 crystallites. At 20°C, O_2 chemisorption on (Co)MoS_2/alumina also leads to displacement of the terminal Co–S bond and the formation of one Co–O bond at a distance of about 2.01(5) Å. The terminal Co–S bond distance is 2.26(2) Å and is significantly longer than the four bridging Mo–S–Co bonds, which are 2.18(2) Å. At 100°C, the latter are unreactive to O_2, although the Co ion coordination increases to about six, i.e., four bridging Co–S and two terminal Co–O bonds. The Co chemisorption results suggest that the terminal Co–S is the reactive bond that has been displaced by the oxygen adsorbate.

Key Words: **hydrodesulfurization; EXAFS; molybdenum; cobalt; CoMo catalyst; HDS catalyst; O_2 chemisorption.**

INTRODUCTION

The sulfur content in crude oil continues to increase both in the United States and throughout the world. At the same time, recent environmental regulations aimed at greatly reducing the amount of sulfur in gasoline and diesel fuels in the United States and Europe have renewed efforts to develop more active and selective catalysts. For example, the average sulfur content of gasoline in the United States is currently around 300 ppm. The regulations of the U.S. Environmental Protection Agency require reducing sulfur in gasoline to 30 ppm by the year 2006 (1). Reducing sulfur to these very low levels without hydrogenating the octane-rich olefin compounds in the gasoline is very difficult. Therefore, a key to the development of improved catalysts is a precise understanding of the structure of the active site, especially during the interaction with reactants and under operating conditions.

Alumina-supported Mo and W sulfide catalysts are widely used in petroleum refining for removal of S and N heteroatoms (2). The activity of MoS_2 catalysts is promoted by addition of Co or Ni, and the structure of the active site has been extensively studied by numerous techniques (2, 3). Mössbauer (4–9) and EXAFS (9–16) analysis have provided the most detailed and complete information about the local structure of the active phase. The catalytic site in (Co)MoS_2 is composed of isolated, five to six S-coordinated Co ions located at the edge of small MoS_2 crystallites (4, 5) and bridging between two Mo atoms (12, 13). While it has been proposed that the catalyst has four bridging Co–S–Mo bonds and one or two terminal Co–S bonds, only one Co–S distance at 2.20 Å has been resolved using standard EXAFS analysis (11, 15, 16).

Chemisorption of adsorbates, like O_2, NO, CO, etc., has often been used to estimate the MoS_2 particle size (2, 3). Oxygen selectively chemisorbs at the MoS_2 edge (17–21), and the adsorption capacity increases linearly with the Mo loading (18). Although the adsorption stoichiometry has not been firmly established and every active site may not be titrated (20, 22–25), oxygen is thought to chemisorb only at the catalytic site (17–20, 26–29). Thus, determination of the changes in structure that occur during adsorption and reaction with oxygen could provide insight into the important steps in the catalytic cycle.

This paper describes the changes that occur at the Co and Mo atoms of a (Co)MoS_2/alumina catalyst after adsorption and partial oxidation with O_2. Since the changes to the catalytic surface that occur are relatively small, a modified EXAFS analysis procedure has been adopted. On the basis of this analysis, two Co–S distances have now been resolved,

[1] To whom correspondence should be addressed. E-mail: millejt1@bp.com.

0021-9517/01 $35.00

while at the Mo ions, oxidation leads to replacement of a portion of the bridging S by O ions.

EXPERIMENTAL

Catalysts. Catapal SB alumina was calcined at 500°C. The alumina support was impregnated with ammonium heptamolybdate (Aldrich) to give 5 wt% Mo, dried overnight at 100°C, and calcined at 350°C. The CoMo/alumina catalyst, KF-756 from Akzo Nobel, was commercially available and contained 11.2% Mo and 3.1% Co. The catalysts were presulfided at atmospheric pressure by heating in a high flow (20 cm^3/min per gram of catalyst) of 5% H_2S in H_2. The sulfiding temperature was increased from room temperature to 350°C at 5°C/min, held at 350°C for 2 h, and cooled to room temperature in H_2S/H_2.

Oxygen chemisorption. Prior to the chemisorption determination, the presulfided MoS_2/alumina catalyst was reduced in static H_2 and evacuated at 350°C. The O_2 chemisorption was determined by the double isotherm method and extrapolated to zero partial pressure (17).

EXAFS data collection. The EXAFS measurements were made on the insertion device beam line of the Materials Research Collaborative Access Team (MRCAT) at the Advanced Photon Source, Argonne National Laboratory. Measurements were made in transmission mode with the ionization chambers optimized for maximum current with linear response. A double-crystal Si (111) monochromator with resolution ($\Delta E/E$) better than 2×10^{-4} at 20 keV (~4 eV) was used in conjunction with a Pt-coated mirror to minimize the presence of harmonics (30). The integration time per data point was 1–3 s and three scans were obtained for each processing condition.

The sample thickness was chosen to give an absorption edge step ($\Delta\mu x$) of about 1.0 in the Mo edge region: approximately 0.5 g of presulfided MoS_2/alumina, or 0.2 g of (Co)MoS_2/alumina. The sample was centered in a continuous-flow *in situ* EXAFS reactor vessel (45 cm long by 2 cm diameter) fitted with Kapton windows. Due to the strong absorption of the Mo and the support in the CoMo/alumina catalyst, at the Co K-edge (7.709 keV) extra care was taken to provide a uniform sample as well as to eliminate higher order harmonics in the beam. To assure uniformity, the finely ground sample (<100 mesh) was pressed into a wafer between polished steel dies. The Co absorption edge step was $\Delta\mu x = 0.6$ with a total sample absorption $\mu x \sim 3.5$ above the edge. The Co edge data range was limited to 12.5 $Å^{-1}$ due to the presence of Ni impurities in the sample.

Standard procedures were used to extract the EXAFS data from the absorption spectra using WINXAS97 software (31). Prior to the EXAFS measurements, the presulfided catalysts were heated to 350°C for 1 h at atmospheric pressure in a flow of 5% H_2 in He (150 cm^3/min). The EXAFS data were collected at room temperature in 5% H_2/He. Additionally, following reduction and after purging at room temperature with He, the catalyst was treated in 5% O_2/He at room temperature or 100°C. The EXAFS data were collected at room temperature in 5% O_2/He.

Phase shift and backscattering amplitudes were obtained from reference compounds: MoS_2 for Mo–S and Mo–Mo (32), Na_2MoO_4 for Mo–O (33), CoS_2 for Co–S (34), and CoO for Co–O (35).

Data analysis by difference method. The EXAFS signal is composed of a linear combination of the absorption fine structure of each scattering path in the sample (36). To a first approximation (ignoring electronic changes), removing/adding one coordinating atom from the environment of one absorbing atom will eliminate/add the scattering path from that pair of atoms, resulting in an immeasurably small change in the EXAFS. The difference method extends this idea to larger changes. In the case of MoS_2, if oxygen is adsorbed to the edge of the MoS_2 particles at the exposed Mo sites, then additional scattering paths will contribute to the signal. The impact on the EXAFS will be proportional to the number of Mo–O bonds formed. In small enough particles, where there is a large fraction of surface-exposed Mo atoms, the adsorption of oxygen will have a measurable effect. If two scans of the same sample differ by a small amount, subtracting one spectrum from another will result in a data set that describes the difference between the state of the sample in the two scans. Furthermore, the difference may be analyzed by standard analysis methods.

In the hypothetical example chosen, if adsorption has no effect on the structure of MoS_2, the EXAFS measured from the core catalyst particle would be identical before and after adsorption of oxygen, the only change being the addition of the adsorbed Mo–O scattering paths. Therefore, taking the difference of the two spectra before and after oxidation would leave only that contribution due to the added Mo–O paths (within a single scattering approximation). It will be shown later that oxygen adsorption, even at 20°C, has a small effect beyond adding Mo–O bonds.

A second possibility is illustrated for the Co coordination environment in (Co)MoS_2. The EXAFS spectra were measured after reducing/sulfiding the catalyst (scan A) and again after exposure to oxygen (scan B). If an oxygen atom were to replace a sulfur atom in the coordination sphere of Co, fitting the difference signal, given by scan A minus scan B, would result in measuring one sulfur path and one (negative amplitude) oxygen path. The advantage of this technique is clearly that it emphasizes the signal from the new coordinating atom. In general, conventional analysis methods that use nonlinear fitting algorithms are inadequate for fitting a small-amplitude path in the presence of a much larger amplitude path, while still obtaining meaningful fitting results and uncertainties. In most cases, the

value of χ^2 is minimized with respect to variations in the fit parameters. The contribution of one Co–O path per Co atom is very small compared with the five or six Co–S paths, which overlap in the Fourier transform. Using conventional analysis techniques, changes to the fitting parameters for the Co–O path have very little effect on the χ^2 value, even when parameters for the Co–O path are not highly correlated with other fit parameters. It becomes very difficult to assign any significance to the results when the additional path is included.

The process by which the difference spectrum can be obtained is straightforward. The critical step is the energy calibration. A reference spectrum must be taken simultaneously with the scan of the catalyst, from which the energy calibration can be verified if there can be more than a 0.1 eV drift in the calibration of the monochromator. The scans must be on the same energy scale (at least near the edge) to within 0.1–0.2 eV. The data should then have the pre-edge background removed and be normalized to an edge step, $\Delta\mu x$, equal to one, as is conventional. At this point, the raw data from one scan may be subtracted from another, with interpolation of the data points to a common grid if necessary. The background removal function may then be applied. Alternatively, the background may be removed, the data converted to k-space, and then the subtraction performed. In this case, the same edge energy (E_0) must be used for all scans to calculate the electron momentum wavenumber, k; otherwise, significant artifacts will be introduced into the difference spectra. However, taking the difference of the raw data before subtracting the slowly varying background function will result in a data range significantly extended to lower k values; this capability may be important for data sets with a limited range, or samples with low-Z backscatterers, such as oxygen.

Methods of isolating shells of interest by using restricted data ranges (in r- or k-space) or different k-weightings to emphasize different backscatters are applicable to most problems, and are a common technique used to fit EXAFS data. It should be noted that this method, while conceptually similar to other methods that attempt to improve the statistical significance of one path by removing another path from the data (37), is actually quite different. This method is based on the physical similarities and differences of a sample in two spectra. The difference is a model-independent method of isolating changes between two different scans and may only be used in a limited class of experiments. Ramaker *et al.* have used a similar method to analyze the L_3 and L_2 near-edge spectra of Pt metal catalysts on γ-Al_2O_3 supports (38).

The difference data set may now be analyzed by standard techniques, with one difference. Instead of positive definite coordination numbers, the coordination number for a path may now be positive or negative. This procedure has been verified for the one set of conditions in which it was possible to fit directly each data set individually as well as use the difference technique, i.e., the difference between the reduced MoS_2 catalyst and the same sample oxidized at 100°C.

The experimental and theoretical difficulty can be expressed with two questions: how much change in the overall structure may be considered small, and how small a difference is significant? To address the first question consider the following. First, small changes in either radial distance or the energy origin will result in a difference signal that looks similar to the derivative of the original signal, with the amplitude increasing for increasingly larger changes. Second, changes in coordination number alone will look like the expected EXAFS signal for a single path. Third, small changes in the EXAFS Debye–Waller factor will look similar to changes in the coordination number, but will have nearly zero amplitude at low k values with increasing amplitude at larger k values. As a result, the difference method, in the form presented here, may only be used to measure changes in the constituents of the coordination environment. It must be used with care if there are other significant changes to the structure.

To examine the effects of small changes in the bulk structure, several simulations were run that systematically investigated the effect of differences in the radial distance, energy origin, EXAFS Debye–Waller factor, and coordination number (i.e., R, E_0, σ^2, and N, respectively) on the EXAFS from the first two shells of MoS_2. These simulations were based on scattering paths calculated using *feff* version 8.0 (39), while the simulated data were produced from these scattering paths using *feffit* (40). Figure 1 shows the simulation results for changes in the distance of the Mo–S path as well as changes in the edge energy, due to either incorrect calibration or a chemical shift. Both variables affect the phase of the $\chi(k)$ data. In Fig. 1a.i, E_0 is shifted by +2 eV. Even this small shift produces significant differences between the two data sets (solid line), although the changes are more pronounced at low k, since k^2 is proportional to $E - E_0$ [i.e., $\hbar^2k^2 = 2m_e(E - E_0)$]. In addition, the difference is similar to the negative derivative of the original data. The amplitude of the Fourier transform of the difference is about 20% as large as the original data (Fig. 1b). Shifts in E_0 cause the imaginary component of the Fourier transform to also look like a derivative of the original data, although the peaks in the magnitude still roughly line up with the original data (slightly shifted to lower R). Clearly, the energy calibration is important, as are potential chemical shifts. If possible, the calibration should be maintained to 0.1–0.2 eV to minimize this effect.

Figure 1a.ii shows the effect of changing the Mo–S bond length, R_{Mo-S}, by 0.02 Å for all Mo–S pairs. For clarity, only the Mo–S path is shown (dotted line) and not the entire spectrum. The solid line is the difference. Once again, the difference looks like a derivative of the original signal, but

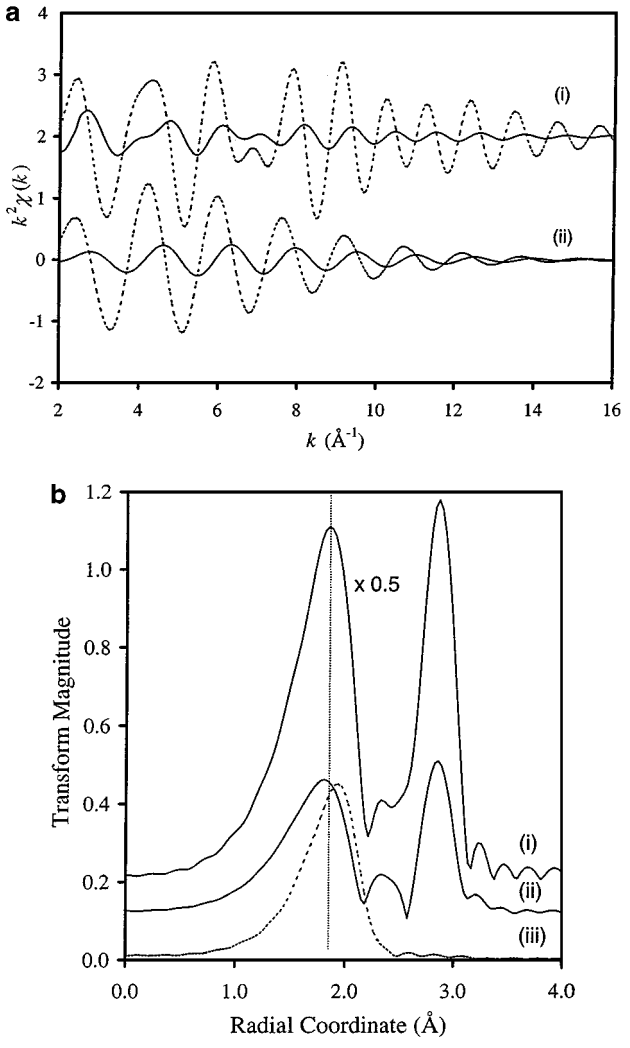

FIG. 1. (a) A simulation of the EXAFS for a change in E_0 and the bond length of the Mo–S path. (i) k^2-weighted $\chi(k)$ simulation of MoS_2 (dashed line) and the difference between the simulated spectrum (i) and the spectrum with E_0 shifted by +2 eV (solid line). (ii) k^2-weighted $\chi(k)$ simulation of the Mo–S path (dashed line), and the difference between the simulated spectrum (i) and the spectrum with Mo–S bond length decreased by 0.02 Å (solid line). (b) Magnitude of the Fourier transform of the (i) simulated data for MoS_2, (ii) the difference spectrum for a +2 eV difference in E_0, and (iii) the difference spectrum for a −0.02 Å change in the Mo–S bond length. The transform was taken with $\Delta k = 2$–15 Å^{-1}. The vertical dashed line marks the position of the MoS_2, Mo–S peak.

in contrast to changes in E_0, the difference is relatively small at low k and increases at higher k. A change of 0.02 Å causes the amplitude of the difference to be about 20% of the original. The amplitude is roughly proportional to the change in the bond length. To have a negligible impact on the difference spectrum, the changes in bond lengths should be less than 0.002 Å. However, since changes in bond length are easily distinguishable from changes in coordination number, the maximum difference that can be tolerated depends on the magnitude of the effect one is studying. In this case, changes in the bond distances of as much as 0.005 Å would not significantly alter the results.

Changes in the coordination number or the Debye–Waller factor cause the difference spectrum to be in-phase with a particular path in the original spectrum. Since the DW factor has little effect on the EXAFS at low k, the difference is also close to zero at low k, with increasing amplitude relative to the original data at high k. A change in coordination number clearly results in a path identical to the original path, only with smaller amplitude. In the case of MoS_2, a change of 20% in the coordination number results in a difference spectrum that has an amplitude similar to a change of 0.002 Å^2 in the DW factor. Therefore, in order to be negligible, DW factor changes must be smaller than ca. 5×10^{-4} Å^2.

The second question is that of how small a difference may be considered significant. Since the magnitude of a real structural difference that can be detected depends to a large degree on the quality of the data and the experimental conditions, this cannot be answered generally. In these measurements, it is clear that the difference spectrum reflects changes in the Mo–Mo coordination number as small as 0.2 and that this difference is significantly larger than the noise level (see Fig. 8). Nonetheless, given the complication of changes in other variables (i.e., E_0, R, and σ^2), it is not entirely clear whether this small difference reflects a real change in the coordination number.

RESULTS

MoS_2/Alumina

The catalytic properties, chemical analysis, surface area, X-ray diffraction, and EXAFS analysis of the sulfided MoS_2/alumina catalyst have previously been given (16). The elemental analysis is 4.5 wt% Mo, and the O_2 chemisorption capacity at 20°C is 1.87 cm^3/g, or a 0.36 O/Mo molar ratio.

Figure 2 shows the changes in the k^2-weighted EXAFS data and the magnitude of the Fourier transform of the MoS_2/alumina catalyst exposed to 5% O_2 at 20°C and 100°C. Adsorption of O_2 at 20°C leads to small changes in the EXAFS data. The Fourier transform shows a small increase in the shoulder on the low-R side of the Mo–S peak at about 2 Å. Only minor changes in the Mo–S and Mo–Mo coordination numbers occur on chemisorption of O_2. Heating the MoS_2/alumina catalyst in 5% O_2 at 100°C leads to larger changes in the EXAFS data, with a distinctive Mo–O peak at about 1.5 Å in the uncorrected Fourier transform. Additionally, both the Mo–S and Mo–Mo peaks at around 2 Å and 3 Å, respectively, decrease slightly in the Fourier transform.

Because of the large and partially resolved Mo–O coordination in the MoS_2/alumina catalyst oxidized at 100°C, the spectrum could be fit with moderate success by standard

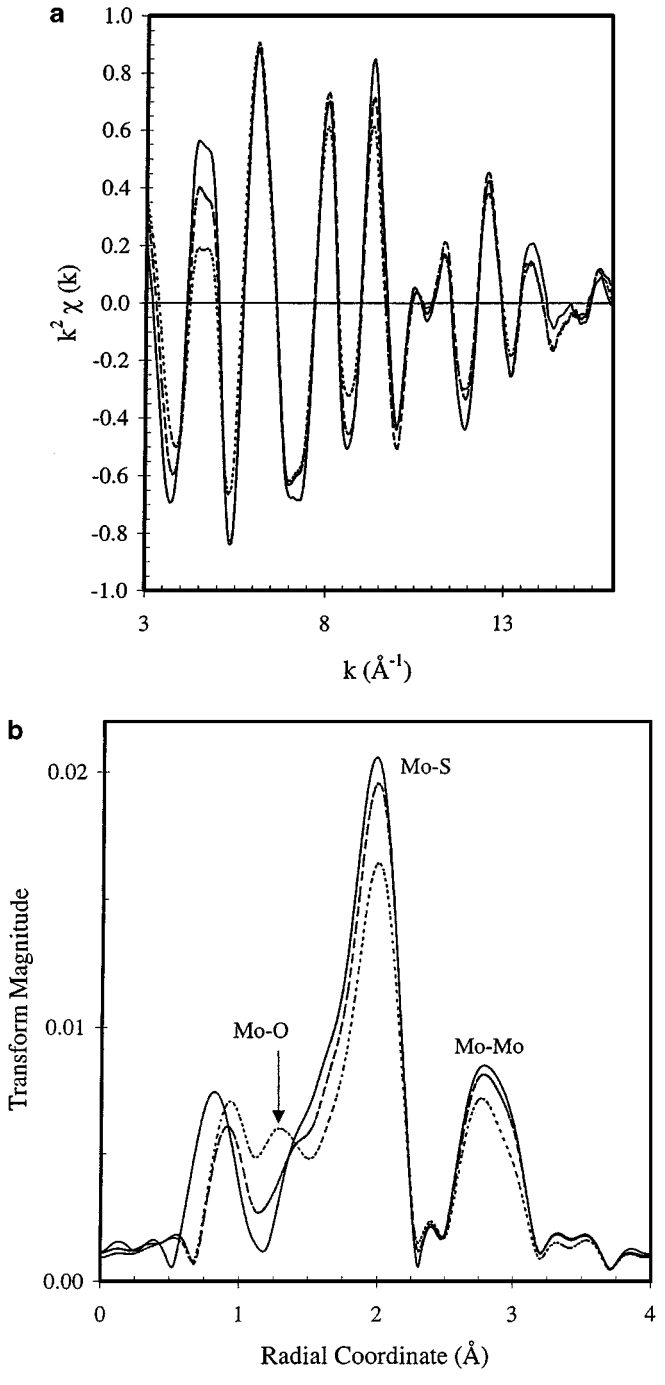

FIG. 2. Molybdenum K-edge EXAFS data for sulfided MoS_2/Al_2O_3 (solid line, sulfided; dashed line, sulfided followed by 5% O_2 at 20°C; and dotted line, sulfided followed by 5% O_2 at 100°C). (a) k^2-weighted raw data and (b) magnitude of the k^2-weighted Fourier transforms, $\Delta k = 3.10$–16.02 Å^{-1}.

procedures. The three-shell model fit (Mo–O, Mo–S, and Mo–Mo) to the isolated EXAFS data for the 100°C oxidized MoS_2/alumina catalyst is shown in Fig. 3, and the coordination parameters are given in Table 1 along with those previously given for the sulfided catalyst (16). At 100°C, the Mo–O coordination number, N_{Mo-O}, is 0.8 at a distance of 1.69 Å, which is significantly shorter than the 1.77 Å in Na_2MoO_4, i.e., Mo^{6+}–O (33), but is similar to two of the tetrahedral Mo^{6+}–O bonds in $CoMoO_4$, i.e., 1.72 Å. Also, there is a decrease of about 0.9 and 0.3 in N_{Mo-S} and N_{Mo-Mo}, respectively. The replacement of Mo–S by Mo–O disrupts the MoS_2 structure, as evidenced by the smaller Mo–Mo coordination; however, much of the MoS_2 structure remains unchanged.

While the EXAFS spectrum of catalyst oxidized at 100°C could be fit by standard analysis procedures, the spectrum for MoS_2/alumina exposed to oxygen at 20°C could not. All attempts to determine a Mo–O contribution were unsuccessful due to the large, overlapping Mo–S path, which dominated the fit. The small changes, however, could be fit by analysis of the difference spectrum between the sulfided catalyst and the catalyst with oxygen.

The validity of the difference method was verified by comparing the results with those of the standard analysis for MoS_2/alumina oxidized at 100°C. The multiple-shell, *R*-space fit of the Fourier transform of the difference spectrum for the MoS_2/alumina catalyst minus that oxidized at 100°C is shown in Fig. 4 along with the three-shell model fit. Since the Mo–S path in the difference spectrum is much smaller than in the direct fit of the sulfided catalyst, the Mo–O path is better resolved from the Mo–S path. The fitting parameters for the difference spectrum are given in Table 1, and indicates about 0.7 fewer Mo–S and 0.3 fewer Mo–Mo, in good agreement with the difference in coordination parameters determined by direct fitting of the sulfided and

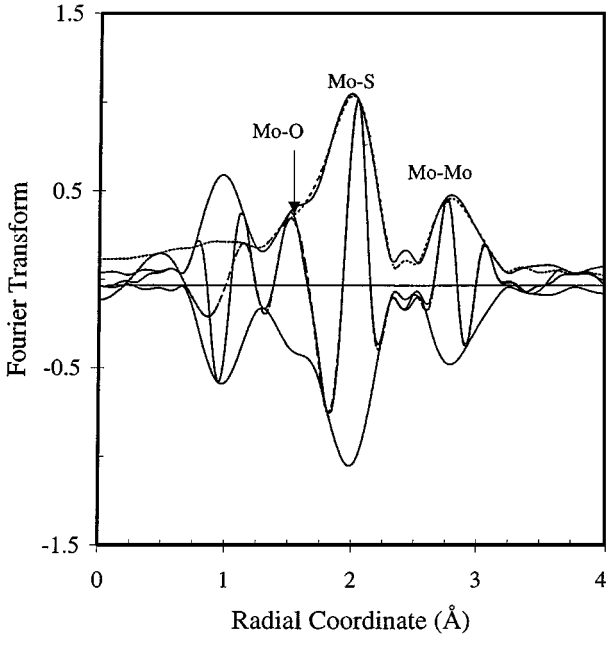

FIG. 3. Three-shell, *R*-space (direct) model fit: Mo K-edge EXAFS data for sulfided MoS_2/Al_2O_3 followed by 5% O_2 at 100°C, k^2, $\Delta k = 2.95$–16.04 Å^{-1}, $\Delta R = 1.17$–3.15 Å; solid line, data; dotted line, model fit.

TABLE 1

EXAFS Analysis of MoS_2/Alumina + O_2: Mo Edge

Path	Δk, Å^{-1}	ΔR, Å	N(Coord. number)	R, Å	$\Delta\sigma^2$, Å^2($\times 10^{-3}$)	ΔE_o, eV
Sulfided: Multiple-Shell Fit of k^2-Weighted Fourier Transform						
Mo–S	2.95–16.04	1.25–3.16	3.6(3)	2.42(1)	2.0	−0.2
Mo–Mo			1.9(2)	3.15(2)	2.2	−1.0
Sulfided + O_2 at 20°C: Multiple-Shell Fit of k^2-Weighted Fourier Transform of the Difference Spectrum[a]						
Mo–S	2.95–12.01	1.13–3.17	0.2(2)	2.42(3)	2.0	−3.5
Mo–Mo			0.2(2)	3.18(3)	3.8	−5.0
Mo–O			−0.5(2)	1.72(2)	5.0	5.1
Sulfided + O_2 at 100°C: Multiple-Shell Fit of k^2-Weighted Fourier Transform of the Difference Spectrum[a]						
Mo–S	2.95–15.12	1.02–3.23	0.7(2)	2.42(2)	1.9	1.8
Mo–Mo			0.3(2)	3.16(2)	1.3	0.8
Mo–O			−1.2(3)	1.73(2)	6.4	5.8
Sulfided + O_2 at 100°C: Multiple-Shell Fit of k^2-Weighted Fourier Transform						
Mo–S	2.95–16.04	1.17–3.15	2.7(3)	2.42(1)	2.0	−1.1
Mo–Mo			1.6(2)	3.14(2)	1.8	−0.2
Mo–O			0.8(2)	1.69(3)	1.7	5.1

[a] In the difference spectra, a positive sign indicates a net loss while a negative sign indicates a net gain in the coordination number (N) of the oxidized samples.

100°C oxidized catalysts. The Mo–O coordination number (1.2) is larger than the direct fit and the bond distance is somewhat larger (1.73 Å) in the difference spectrum. This difference is due to the correlation between the DW factor and the coordination number. Na_2MoO_4, the standard used for the Mo–O path, has an unusually low DW factor, about 1.4×10^{-3} Å^2 (from fitting to *feff* calculations). Therefore, the Mo–O DW factor in the difference fits is actually in a range more typical of O nearest neighbors. Due to the better resolution of the Mo–O contribution, the results obtained by analyzing the difference spectrum are the more accurate.

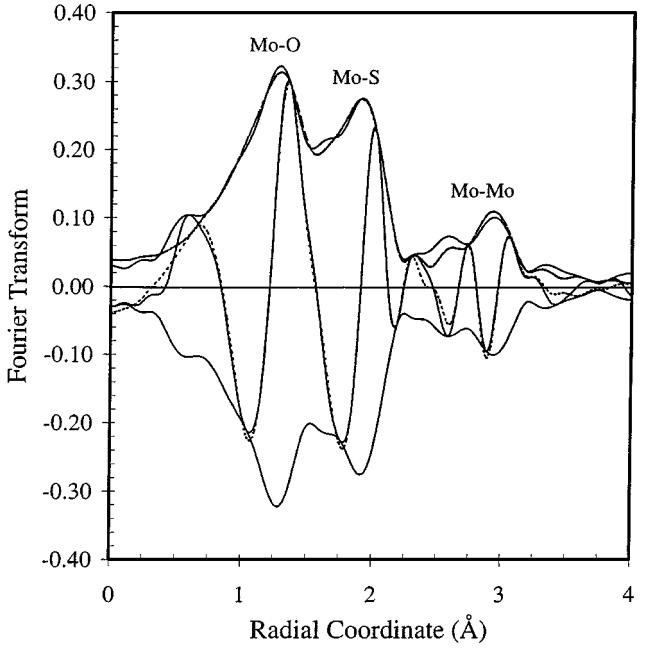

FIG. 4. Three-shell, R-space model fit: Mo K-edge EXAFS for difference spectrum of sulfided MoS_2/Al_2O_3 minus sulfided MoS_2/Al_2O_3 followed by 5% O_2 at 100°C, k^2, Δk = 2.95–15.12 Å^{-1}, ΔR = 1.02–3.23 Å; solid line, data; dotted line, model fit.

While the Mo–O path is barely visible in the Fourier transform of the MoS_2/alumina with adsorbed O_2 at 20°C, Fig. 2b (dashed line), the Mo–O path is well resolved in the Fourier transform of the difference (not shown), and the fit results are given in Table 1. At 20°C, N_{Mo-O} is 0.5 at a bond distance of 1.72 Å, which is within experimental error of the O_2 chemisorption value of 0.36 O/Mo. There are only minor changes in the Mo–S (0.2) and Mo–Mo (0.2) coordination numbers. At 20°C, therefore, oxygen is most likely chemisorbed at the edges of the MoS_2 sheets with little change in the MoS_2 structure.

(Co)MoS_2/Alumina Catalyst

The catalytic properties, chemical analysis, surface area, X-ray diffraction, and EXAFS analysis of the (Co)MoS_2/alumina catalyst have previously been given (16). The sulfided CoMo/alumina catalyst was also treated with O_2 at 20°C and 100°C, and the EXAFS spectra were measured at both the Mo and Co edges. While small changes were observed in the raw data and Fourier transforms in both edges following treatment with O_2 (not shown), none of the spectra could be fit directly. Analysis of the difference, however, gave satisfactory fits even for very small changes due to chemisorbed oxygen. Typical fits of the (Co)MoS_2/alumina catalyst treated in O_2 at 20°C are shown in Figs. 5 and 6 for the Mo and Co edges, respectively. The coordination parameters for the model fits at the Mo

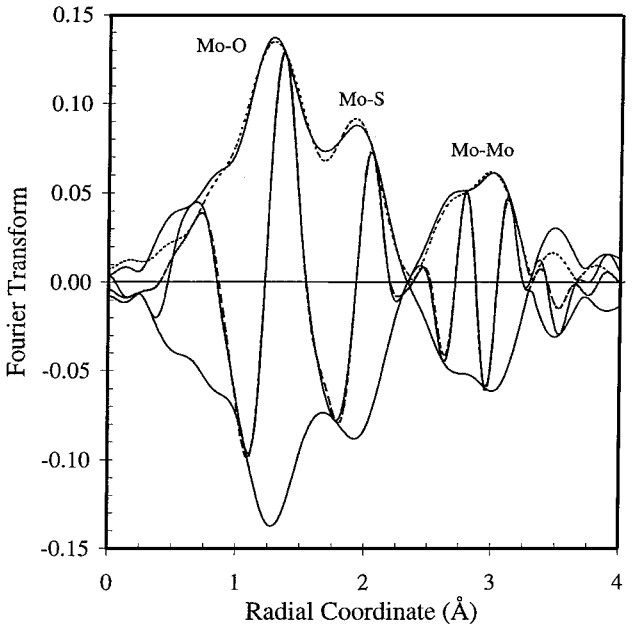

FIG. 5. Three-shell, *R*-space model fit: Mo K-edge EXAFS for difference spectrum of sulfided (Co)MoS_2/Al_2O_3 minus sulfided (Co)MoS_2/alumina followed by 5% O_2 at 20°C, k^2, $\Delta k = 3.15$–12.51 Å^{-1}, $\Delta R =$ 1.04–3.34 Å; solid line, data; dotted line, model fit.

edge are given in Table 2, and those for the Co edge in Table 3.

At the Mo edge of the (Co)MoS_2/alumina catalyst treated with O_2 at 20°C, the Mo–O coordination number is 0.7 at a distance of 1.74 Å, with small changes in N_{Mo-S} and N_{Mo-Mo} of 0.1 and 0.2, respectively. As the temperature of the O_2 treatment increases to 100°C, N_{Mo-O} increases to 1.1 bonds at a distance of 1.72 Å. In addition, there is a further decrease in the N_{Mo-S} (0.7) and N_{Mo-Mo} (0.3). As observed for MoS_2/alumina, at 20°C oxygen is chemisorbed with little oxidation of the MoS_2 crystallites, while at 100°C the decrease in the Mo–S coordination and replacement by Mo–O suggests a partial disruption of the (Co)MoS_2 particles.

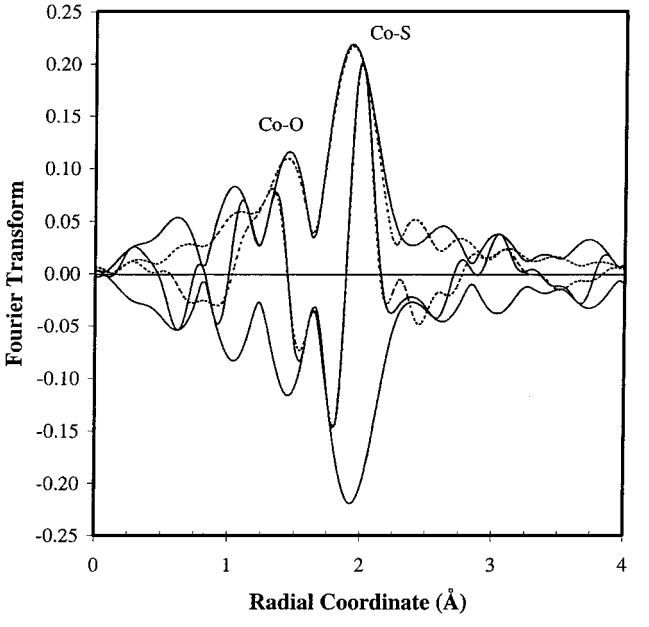

FIG. 6. Two-shell, *R*-space model fit: Co K-edge EXAFS for difference spectrum of sulfided (Co)MoS_2/Al_2O_3 minus sulfided (Co)MoS_2/Al_2O_3 followed by 5% O_2 at 20°C, k^2, $\Delta k = 2.85$–10.83 Å^{-1}, $\Delta R = 1.09$–2.37 Å; solid line, data; dotted line, model fit.

At the Co edge, O_2 at 20°C leads to the formation of a Co–O bond, 1.2 per Co, at a distance of 2.00 Å, which is considerably shorter than the 2.13 Å bond in CoO (34), but similar to the distances in octahedral Co^{2+}–O in $CoMoO_4$, ca. 2.00–2.06 Å. At the same time, there is a decrease in the Co–S coordination number by 0.6 at a Co–S distance of 2.26 Å. The Co–S bond, which has been displaced by oxygen, is longer than the average Co–S distance in the sulfided (Co)MoS_2/alumina catalyst, which is 2.20 Å. At 100°C, there is a further increase in the Co–O coordination, to 1.9 at a distance of 2.01 Å, and a small additional decrease in the N_{Co-S}, to 1.1 less than the reduced catalyst at a distance of 2.25 Å.

Figure 7 shows the near edge spectra for the Co edge. It is clear from the increase in the white-line intensity and the small increase in the edge energy that the Co has been oxidized. Although it is not an easily quantifiable measure of the oxygen coordination, the magnitude of the white-line intensity increase qualitatively corresponds to the results we measure in the difference spectra.

DISCUSSION

EXAFS Analysis

In general, the small changes in the structure due to chemisorption and low-temperature oxidation by O_2 could not be determined by fitting the data directly. The small metal–oxygen coordination is dominated by the larger, overlapping metal–sulfide coordination; therefore, an alternative fitting procedure was adopted. Since the changes in structure due to exposure by oxygen were small, fits were made to the difference of two spectra, i.e., EXAFS data for the sulfided catalyst minus those for the sulfided catalyst plus oxygen. Attempts to subtract the isolated shells gave inconsistent results since selection of the correct data range was not obvious and, generally, overlapped with other features. Subtraction of the entire EXAFS spectra or, alternatively, subtraction of the normalized edge spectra gave reliable difference spectra. Once the difference spectrum has been obtained, it can be analyzed by standard procedures to determine the coordination parameters.

In the difference spectra, the Mo–S and Mo–Mo (and Co–S) coordinations, which are larger in the sulfided catalyst, occur as normal peaks and can be fit with the same phase and amplitude reference functions. However, the Mo–O (and Co–O) paths in the difference spectra are

TABLE 2

EXAFS Analysis of (Co)MoS_2/Alumina + O_2: Mo Edge

Path	Δk, Å^{-1}	ΔR, Å	N(Coord. number)	R, Å	$\Delta\sigma^2$, Å^2($\times 10^{-3}$)	ΔE_o, eV
Sulfided: Multiple-Shell Fit of k^2-Weighted Fourier Transform						
Mo–S	2.99–16.04	1.08–3.20	5.8(3)	2.42(1)	2.1	−0.8
Mo–Mo			2.9(3)	3.16(2)	2.2	0.8
Sulfided + O_2 at 20°C: Multiple-Shell Fit of k^2-Weighted Fourier Transform of the Difference Spectrum[a]						
Mo–S	3.15–12.51	1.04–3.34	0.2(2)	2.46(3)	2.6	3.6
Mo–Mo			0.1(2)	3.20(4)	0.5	0.9
Mo–O			−0.7(2)	1.74(2)	9.2	6.5
Sulfided + O_2 at 100°C: Multiple-Shell Fit of k^2-Weighted Fourier Transform of the Difference Spectrum[a]						
Mo–S	3.16–12.77	0.88–3.28	0.7(2)	2.40(2)	2.6	2.3
Mo–Mo			0.3(2)	3.18(2)	1.8	3.4
Mo–O			−1.1(2)	1.72(2)	7.6	4.5

[a] In the difference spectra, a positive sign indicates a net loss while a negative sign indicates a net gain in the coordination number (N) of the oxidized samples.

present in the oxidized sample and require fitting with a reference phase function that is 180° out of phase from the normal reference, with the effect of inverting the signal. The amplitude function is identical to the standard reference.

In a typical EXAFS experiment, the coordination number may not be known to better than ±10%. This limit is imposed by a lack of detailed knowledge of the backscattering amplitude function, as well as possible systematic errors that affect the amplitude of the EXAFS signal. These include a variety of sample thickness effects, as well as the electronics' response characteristics. When data are compared from two similar samples taken under similar conditions, the backscattering amplitude transferability is improved, and many of the systematic effects can be ignored.

In these experiments, the sample is nearly identical from scan to scan, except for the changes induced by oxidation and small shifts in the sample position in the X-ray beam. Under these circumstances, the relative error in the coordination number between two data sets is much lower: certainly better than 5% of the total amplitude. Based on this, an estimate of the coordination number error in the difference spectrum would be ±0.3 for small changes. The actual uncertainty could be somewhat lower. Data on these catalysts taken during different runs, or taken one after the other, all show no evidence of anomalous peaks in the Fourier transform of the difference spectra. Lines iv in Figs. 8a and 8b show $\chi(k)$ and the Fourier transform of the difference between two spectra taken consecutively on the same reduced MoS_2 sample. Essentially no difference is apparent between the two data sets, and the Fourier transform shows only a hint of a peak. The smallest differences occur between the reduced catalysts and those oxidized at 20°C. Figure 8, line iii, shows the difference spectrum for these conditions. The signal is certainly much larger than

TABLE 3

EXAFS Analysis of (Co)MoS_2/Alumina + O_2: Co Edge

Path	Δk, Å^{-1}	ΔR, Å	N(Coord. number)	R, Å	$\Delta\sigma^2$, Å^2($\times 10^{-3}$)	ΔE_o, eV
Sulfided: Multiple-Shell Fit of k^2-Weighted Fourier Transform						
Co–S	2.80–10.84	1.14–2.23	4.9(5)	2.20(2)	5.0	−5.6
Co–Mo		2.30–2.86	1.1(4)	2.80(4)	10.0	−2.1
Sulfided + O_2 at 20°C: Multiple-Shell Fit of k^2-Weighted Fourier Transform of the Difference Spectrum[a]						
Co–S	2.85–10.83	1.09–2.37	0.6(3)	2.26(3)	1.5	1.7
Co–O			−1.2(4)	2.00(5)	0.4	−2.5
Sulfided + O_2 at 100°C: Multiple-Shell Fit of k^2-Weighted Fourier Transform of the Difference Spectrum[a]						
Co–S	2.85–10.85	1.09–2.37	1.1(4)	2.25(3)	2.2	−0.4
Co–O			−1.9(6)	2.01(5)	−0.4	−3.4
Sulfided: Two-Shell Simulation of k^2-Weighted Fourier Transform						
Co–S	2.80–10.84	1.14–2.23	3.9(4)	2.18(2)	6.3	−8.5
Co–S			1.0[b]	2.26[b]	1.5[b]	1.7[b]

[a] In the difference spectra, a positive sign indicates a net loss while a negative sign indicates a net gain in the coordination number (N) of the oxidized samples.

[b] Coordination parameters fixed in model fit assuming one terminal Co–S and with other parameters determined from the catalyst with O_2 at 20°C.

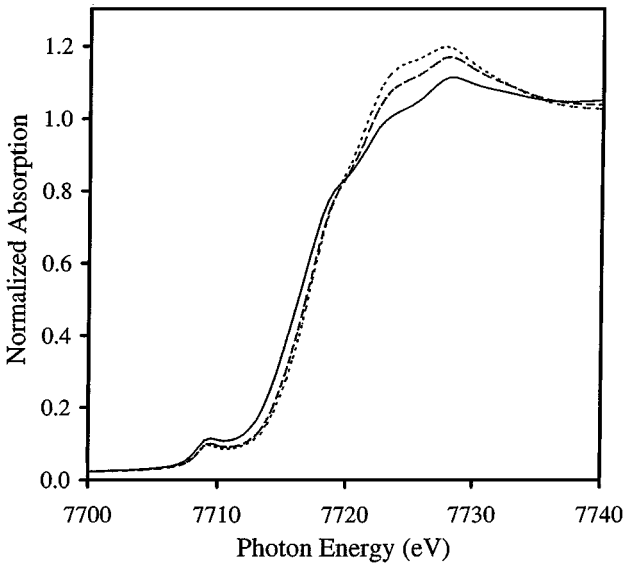

FIG. 7. Normalized Co K-edge adsorption spectra: solid line, sulfided catalyst; dotted line, sulfided $+O_2$ at 20°C; dashed, O_2 at 100°C.

the noise (from scan-to-scan variation). A more detailed analysis suggests that the differences are not primarily due to E_0 shifts, DW factor changes, or distance changes. Therefore, these results could be taken as an upper limit to the uncertainty in the difference fit. Therefore, in general we estimate the minimum uncertainty for the difference fit coordination numbers to be ±0.2, or ±20% of the difference, whichever is larger. The full error analysis takes into consideration different data ranges (Δk and ΔR), k weightings, statistical uncertainties, and the correlation between fitting parameters.

Structure of the (Co)MoS_2/Alumina Catalyst and Reactivity to O_2

Previously, EXAFS has been used to determine the structure of supported (Co)MoS_2, (Ni)MoS_2, and (Ni)WS_2 catalysts (9–16). There is general agreement that Mo is present as small MoS_2 particles with isolated Co ions located at the edge with five or six Co–S bonds at a distance of 2.20 Å. The Co–Mo distance of 2.80 Å suggests that Co is bridge-bonded to Mo by S (11, 12, 15, 16). Although the bridging and terminal Co–S coordinations would be expected to have different bond distances, in (Co)MoS_2 catalysts only one Co–S distance has been resolved. For (Ni)WS_2 catalysts, however, there are six Ni–S bonds: four bridging W–S–Ni bonds at 2.22 Å and two terminal Ni–S bonds at 2.32 Å (13). It is generally assumed, therefore, that (Co)MoS_2 and (Ni)MoS_2 catalysts have four bridging Co(Ni)–S bonds at ~2.2 Å and one terminal Co(Ni)–S bond at ~2.3 Å.

As in previous studies, the Co–S coordination number of (Co)MoS_2/alumina is about five, and the bridging and terminal Co–S distances cannot be resolved. In this study, exposure to O_2 at 20°C and 100°C leads to a loss of about one Co–S bond with a distance of 2.26 Å. The latter is consistent with the longer terminal Ni–S bond in (Ni)WS_2 on carbon and alumina supports (13). While the terminal Co–S bond is reactive to O_2, the remaining four are not, even at 100°C, and are likely bridging bonds. The coordination parameters for the bridging Co–S bonds were determined by fitting the Co-edge EXAFS data of the sulfided (Co)MoS_2/alumina catalyst assuming that there are

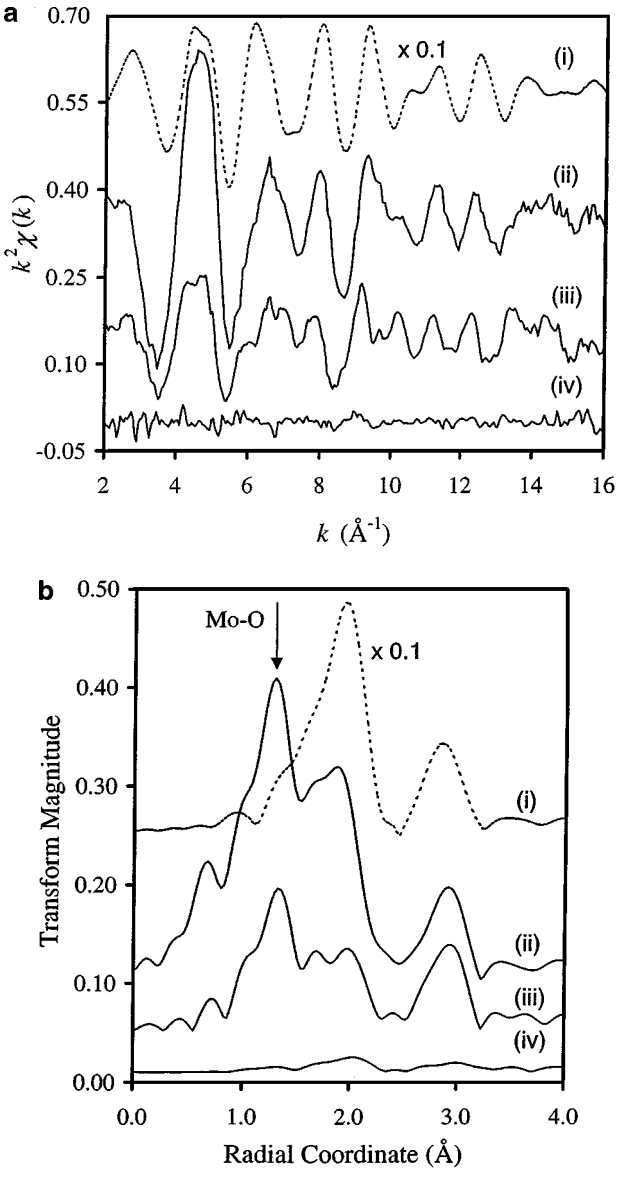

FIG. 8. The (a) $\chi(k)$ and (b) Fourier transform magnitude comparing (i) the reduced MoS_2/Al_2O_3 spectrum (dashed line; amplitude is divided by 10), (ii) the difference between MoS_2/Al_2O_3 oxidized at 100°C and reduced, (iii) the difference between MoS_2/Al_2O_3 oxidized at 20°C and reduced, and (iv) scan-to-scan variation shown by the difference between consecutive scans of reduced MoS_2/Al_2O_3 after calibrating the energy. The arrow in (b) points to the Mo–O peak. (Transform parameters: k^2 weighting, Δk = 2–15 Å^{-1}.)

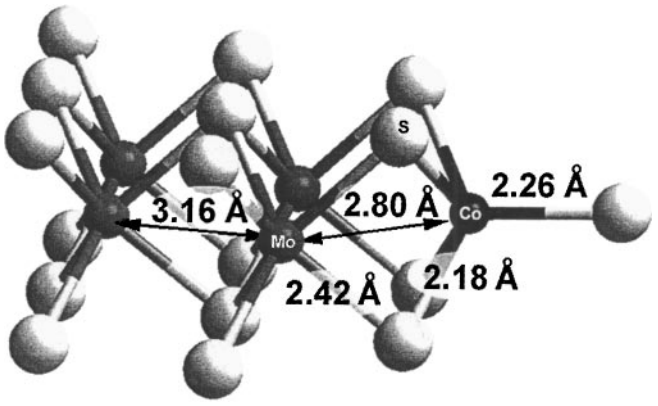

FIG. 9. Molecular model of the local structure of (Co)MoS_2/Al_2O_3.

two Co–S distances. The terminal Co–S bond was assumed to have a distance of 2.26 Å and the other coordination parameters determined from the difference file with O_2 at 20°C. The remaining fit parameters for the bridging Co–S bonds are given in Table 3. There is a good fit with 3.9 (bridging) Co–S at a distance of 2.18 Å, in agreement with the Ni–S distances previously observed for $NiWS_2$ catalysts. It is not possible to determine these Co–S distances directly since the bond length difference is only 0.08 Å, and the large DW factor attenuates the signal very quickly, restricting the practical data range to less than that required to isolate the two shells ($\Delta k \sim 20$ Å^{-1}).

Figure 9 gives the detailed structural model of the (Co)MoS_2/alumina catalyst. While the structural details from O_2 chemisorption confirm that the structures of (Co)MoS_2 and (Ni)WS_2 catalysts are similar, as has been generally assumed, our study also provides additional information about the reactivity of the Co–S bonds. At 20°C, the terminal Co–S is highly reactive to O_2, resulting in the loss of a Co–S bond and the formation of a Co–O bond. The high reactivity of the terminal Co–S bond is also consistent with a recent study on the catalytic conversion of selenophene, a Se analog of thiophene. During catalytic reaction at low temperature, only the terminal Co–S bond was replaced by Co–Se, while the bridging Co–S bonds were reactive only at much higher temperature (15). Thus, the present study and the study of the catalyst under catalytic conditions suggest that the terminal Co–S bond is most reactive.

In the (Co)MoS_2/alumina catalytic process, it is often proposed that a S ion desorbs (or reacts with H_2), generating a coordinately unsaturated site followed by adsorption and reaction (41–49). However, the oxygen chemisorption results suggest another possibility. The terminal Co–S bond was stable to 350°C in H_2 but was rapidly lost at room temperature upon exposure to O_2. This indicates that, at least for O_2, the terminal Co–S is displaced by the adsorbing molecule prior to desorption of S; i.e., a vacant surface site is not required for reaction. A similar proposal was recently suggested for MoS_2/alumina (50). Previously, EXAFS structural analysis under reaction conditions determined that the Mo–S and Co–S coordinations were nearly identical under H_2 and thiophene/H_2, leading to the conclusion that S vacancies are immediately replaced by the reactant (15). The latter result could also mean that the reactant displaces the (terminal) Co–S , and prior desorption is not required.

Finally, at 100°C with O_2, the Co coordination geometry increases from five (five Co–S bonds) to six (four bridging Co–S and two terminal Co–O). These results suggest that the five-coordinate Co is already coordinately unsaturated in the sulfided catalyst. They are also consistent with previous results where N_{Co-S} of (Co)MoS_2/alumina was six when sulfided at 300°C, but decreased to five when reduced under H_2 at the same temperature (15). The latter results suggest that during the catalytic cycle the one terminal Co–S bond in six-coordinate Co is easily lost or displaced, leading to adsorption of the reactant. It is possible that desulfurization proceeds by loss of the second Co–S terminal bond followed by reaction on the same Co atom. While the reaction with O_2 is not a direct study of the HDS (in H_2) catalytic process, it does suggest alternative pathways for adsorption and reaction at the Co atom.

The O_2 chemisorption results for Mo also demonstrate that, although a large fraction of the Co is bonded to the edge of the MoS_2 crystallites, Mo atoms are also exposed to the reactants. For example, at 20°C only minor changes occur to the structure of MoS_2 and the Co–S–Mo bridging bonds. Nevertheless, there is evidence for chemisorption of O_2 and formation of Mo–O bonds. Since the catalytic activity of Co is higher than that of Mo (15, 51–53), de Beer *et al.* have proposed that Co is the active site, and that MoS_2 is required to provide the proper coordination geometry, surface area, and stability (51). Oxygen chemisorption at both the Co and Mo atoms leaves open the possibility that Mo atoms participate in the catalytic cycle (41, 43, 47, 48). However, further studies are required in order to define which atom(s) constitutes the active site.

CONCLUSIONS

The results show that EXAFS analysis of difference spectra is effective for measuring the small changes in catalyst structure due to adsorbates or reactants. This method is probably also applicable to most catalytic studies and should be especially useful for *in situ* studies under reaction conditions.

Analysis of the difference spectra for (Co)MoS_2 on alumina with chemisorbed oxygen indicates that there is one terminal Co–S bond, which is significantly longer (2.26 Å) than the four bridging Co–S bonds (2.18 Å). In addition, the terminal Co–S is reactive to O_2 at 20°C, being displaced by the Co–O bond. By contrast, the bridging Co–S bonds

are unreactive to O_2 at 100°C. Chemisorption of O_2 also indicates that a portion of the Mo atoms at the edge of the MoS_2 crystallites is exposed and may have a role in the catalytic process. At 100°C, sulfur atoms are partially substituted by oxygen in MoS_2, leading to partial disruption of the particles; however, much of the MoS_2 structure remains unchanged.

ACKNOWLEDGMENTS

Use of the Advanced Photon Source was supported by the U.S. Department of Energy, Basic Energy Sciences, Office of Science (DOE-BES-SC), under Contract No. W-31-109-Eng-38. MRCAT is funded by the member institutions and DOE-BES-SC under contracts DE-FG02-94ER45525 and DE-FG02-96ER45589. The authors also thank Kevin Kunz for his assistance in collecting the EXAFS data.

REFERENCES

1. "Control of Air Pollution from New Motor Vehicles: Tier 2 Motor Vehicle Emission Standards and Gasoline Sulfur Control Requirements, Final Rule," Fed. Register, 65 : 28, 6698 (Feb. 10, 2000).
2. Topsøe, H., Massoth, F. E., and Clausen, B. S., *in* "*Catalysis, Science and Technology*" (J. R. Anderson and M. Boudart, Eds.), Vol. II, p. 1. Springer, Berlin, 1996.
3. Eijsbouts, S., *Appl. Catal. A: Gen.* **158**, 53 (1997).
4. Topsøe, H., Clausen B. S., Candia, R., Wivel, C., and Mørup, S., *J. Catal.* **68**, 433 (1981).
5. Wivel, C., Candia, R., Clausen, B. S., Mørup, S., and Topsøe, H., *J. Catal.* **68**, 453 (1981).
6. Wivel, C., Clausen, B. S., Candia, R., Mørup, S., and Topsøe, H., *J. Catal.* **87**, 497 (1984).
7. Crajé, M. W. J., de Beer, V. H. J., and van der Kraan, A. M., *Appl. Catal.* **70**, L7 (1991).
8. Crajé, M. W. J., de Beer, V. H. J., van Veen, J. A. R., and van der Kraan, A. M., *J. Catal.* **143**, 601 (1993).
9. Crajé, M. W. J., Louwers, S. P. A., de Beer, V. H. J., Prins, R., and van der Kraan, A. M., *J. Phys. Chem.* **96**, 5445 (1992).
10. Bouwens, S. M. A. M., Prins, R., de Beer, V. H. J., and Koningsberger, D. C., *J. Phys. Chem.* **94**, 3711 (1990).
11. Bouwens, S. M. A. M., van Veen, J. A. R., Koningsberger, D. C., de Beer, V. H. J., and Prins, R., *J. Phys. Chem.* **95**, 123 (1991).
12. Louwers, S. P. A., and Prins, R., *J. Catal.* **133**, 94 (1992).
13. Louwers, S. P. A., and Prins, R., *J. Catal.* **139**, 525 (1993).
14. Bouwens, S. M. A. M., von Zon, F. B. M., van Dijk, M. P., van der Kraan, A. M., de Beer, V. H. J., van Veen, J. A. R., and Koningsberger, D. C., *J. Phys. Chem.* **146**, 375 (1994).
15. Leliveld, B. R. G., van Dillen, J. A. J., Geus, J. W., Koninigsberger, D. C., and de Boer, M., *J. Phys. Chem. B* **101(51)**, 11160 (1997).
16. Miller, J. T., Reagan, W. J., Kaduk, J. A., Marshall, C. L., and Kropf, A. J., *J. Catal.* **193**, 123 (2000).
17. Tauster, S. J., Pecoraro, T. A., and Chianelli, R. R., *J. Catal.* **63**, 515 (1980).
18. Chung, K. S., and Massoth, F. E., *J. Catal.* **64**, 332 (1980).
19. Tauster, S. J., and Riley, K. L., *J. Catal.* **67**, 250 (1981).
20. Burch, R., and Collins, A., *Appl. Catal.* **17**, 273 (1985).
21. Prada Silvy, R., Delannay, F., Grange, P., and Delmon, B., *Polyhedron* **5**, 195 (1986).
22. Nag, N. K., *J. Catal.* **92**, 813 (1985).
23. Kalthod, D. G., and Weller, S. W., *J. Catal.* **98**, 572 (1986).
24. Topsøe, H., and Clausen, B. S., *Appl. Catal.* **25**, 273 (1986).
25. Moon, S.-J., and Ihm, S.-K., *Appl. Catal.* **42**, 307 (1988).
26. Tauster, S. J., and Riley, K. L., *J. Catal.* **70**, 230 (1981).
27. Bodrero, T. A., Bartholomew, C. H., and Pratt, K. C., *J. Catal.* **78**, 253 (1982).
28. Bodrero, T. A., and Bartholomew, C. H., *J. Catal.* **84**, 145 (1983).
29. Moranda, R., and Kareem, S. A., *Catal. Lett.* **1**, 217 (1988).
30. Segre, C. U., Leyarovska, N. E., Lavender, W. M., Plag, P. W., King, A. S., Kropf, A. J., Bunker, B. A., Kemner, K. M., Dutta, P., Duran, R. S., and Kaduk, J., *in* "CP521, Synchrotron Radiation Instrumentation: 11th U.S. National Conference" (P. Pianetta, *et al.*, Eds.), pp. 419–422. Am. Inst. of Phys., New York, 2000.
31. Ressler, T. J., *J. Phys. IV* **7**, C2-269 (1997).
32. Dickinson, R. G., and Pauling, L., *J. Am. Chem. Soc.* **45**, 1466 (1923).
33. Matsumoto, K., Kobayashi, A., and Sasaki, Y., *Bull. Chem. Soc. Jpn.* **48**, 1009 (1975).
34. Elliott, N., *J. Chem. Phys.* **33**, 903 (1960).
35. *Nat. Bur. Stand. Crit.* **9**, 28 (1959).
36. Koningsberger, D. C., and Prins, R., Eds., "*X-Ray Absorption: Principles, Applications, Techniques of EXAFS, SEXAFS, and XANES.*" Wiley, New York, 1988.
37. Koningsberger, D. C., and Vaarkamp, M., *Physica B* **208 & 209**, 633 (1995).
38. Ramaker, D. E., Mojet, B. L., Oostenbrink, M. T. G., Miller, J. T., and Koningsberger, D. C., *Phys. Chem. Chem. Phys.* **1**, 2293 (1999).
39. Ankudinov, A. L., Ravel, B., Rehr, J. J., and Conradson, S. D., *Phys. Rev. B* **58**, 7565 (1998).
40. Stern, E. A., Newville, M., Ravel, B., Yacoby, Y., and Haskel, D., *Physica B* **208 & 209**, 117 (1995).
41. Roxlo, C. B., Deckman, H. W., Gland, J., Cameron, S. D., and Chianelli, R. R., *Science* **235**, 1629 (1986).
42. Richardson, R. T., *J. Catal.* **112**, 313 (1988).
43. Okamato, Y., Maezawa, A., and Imanaka, T., *J. Catal.* **120**, 29 (1989).
44. Jalowiecki, L., Aboulaz, A., Kasztelan, S., Grimblot, J., and Bonnelle, J. P., *J. Catal.* **120**, 108 (1989).
45. Linder, J., Villa Garcia, M. A., Sachdev, A., and Schwank, J., *J. Catal.* **120**, 487 (1989).
46. Nørskov, J. K., Clausen, B. S., and Topsøe, H., *Catal. Lett.* **13**, 1 (1992).
47. Vrinat, M., Ramirez, J., Breysse, M., Geantet, C., and Massoth, F. E., *Catal. Lett.* **26**, 25 (1994).
48. Mangnus, P. J., Bos, A., and Mouljin J. A., *J. Catal.* **146**, 437 (1994).
49. Helveg, S., Lauritsen, J. V., Laegsgaard, E., Stensgaard, I., Nørskov, J. K., Clausen, B. S., Topsøe, H., and Besenbacher, F., *Phys. Rev. Lett.* **84**(5), 951 (2000).
50. Smit, T. S., and Johnson, K. H., *J. Mol. Catal.* **91**, 207 (1994).
51. de Beer, V. H. J., Duchet, J. C., and Prins, R., *J. Catal.* **72**, 369 (1981).
52. Duchet, J. C., van Oers, E. M., de Beer, V. H. J., and Prins, R., *J. Catal.* **80**, 386 (1983).
53. Vissers, J. P. R., de Beer, V. H. J., and Prins, R., *J. Chem. Soc., Faraday Trans. 1* **83**, 2145 (1987).